

Development of a Feedstock for Additive Manufacturing of 4605 Steel Compact by FDMS Process

Amir Hossein Rahimi¹ · Jamal Zamani¹ 

Received: 4 January 2022 / Accepted: 27 June 2022 / Published online: 30 July 2022
© The Indian Institute of Metals - IIM 2022

Abstract In this study, an optimum feedstock has been developed for additive manufacturing of 4605 steel powder through fused deposition modelling and sintering process using the response surface methodology. For this purpose, 15 feedstock samples containing four part binder system of paraffin wax (PW), polypropylene (PP), carnauba wax (CW), and stearic acid (SA) were compounded with 4605 powder. The rheological, physical and mechanical properties of the samples were measured and optimized with the aim of increasing the strength, density of the final part and reducing the viscosity of the feedstock. The results showed that increase in the percentage of SA and PW reduces the viscosity of the feedstock while increase in PP results in increase in density and strength. Finally, the optimum feedstock is suggested to have 61 wt% of PW, 25 wt% of PP, 10 wt% of CW, and 4 wt% of SA along with 90 wt% of steel powder.

Keywords Feedstock · Fused deposition modelling and sintering · Additive manufacturing · Debinding · Sintering

1 Introduction

Additive manufacturing (AM) is a novel manufacturing technique that due to its many advantages is replacing many traditional techniques specially for low rate production. This method is now being used in many industries like aerospace, automotive, medical, etc. [1]. Amongst all AM

methods, fused deposition modelling and sintering (FDMS) is an economical 3D printing method used for printing of different metals and alloys. This method is a combination of fused deposition modelling (FDM) and powder metallurgy. In brief, the process involves preparation of feedstock, printing the feedstock, debinding (thermal and solution), and sintering. Other metal printing methods are expensive and consume high energy [2]. FDMS has been introduced as an economic, low power consuming method for manufacturing of complex steel parts. In this method, based on FDM, feedstock (raw material that is composed of metallic powder and binder system) is printed layer by layer following a computer-aided design (CAD) model, and then, thermal and solution debinding and later sintering process are conducted on the printed part to prepare a compact alloy part [3]. The journey starts with a CAD system where a 3D model of the final product is designed. The format of the file is later converted to stereolithography (STL) format. The converted file reaches the AM machine (FDM) and is edited accordingly. At the FDM machine, parameters including pressure, energy source, layer thickness, and time are adjusted. Finally, based on the designed model, and the adjusted parameters, the product is printed.

FDMS process variables have significant impact on the performance and quality of the final product [4]. These variables include operational parameters (time, temperature, rotation speed, pressure, solvent type etc.), machine parameters (injection mechanism, heating process, nozzle dimension, printing pattern, printing position on the platform, injection pressure and speed etc.), material parameters (powder type, size, shape, and percentage of the metallic powder along with binder system and its constituents), and geometric parameters of the part to be printed (shape, size, fill percentage).

✉ Jamal Zamani
zamani@kntu.ac.ir

¹ Department of Mechanical Engineering, K.N. Toosi University of Technology, P. O. Box: 19395-1999, Tehran, Iran

The printed green part contains high percentage of binder, and therefore, a debinding process is required. As the hosting matrix of the composition, binders are plastic polymers that adjust the viscosity, avoid buckling and back-flow induced and enhance composite flow ability through the printing process at a certain temperature. Studies report increase in viscosity with the increase in the powder loading of the feedstock and thus recommend the addition of additives to control the flow behaviour of the feedstock melt through the extrusion and printing process [5]. A suitable binder system contains main component, backbone and additives (surfactant, lubricant etc.). Table 1 presents 17 some of the used binder systems in different feedstocks [6].

FDM has been used to deposit liquefied thermoplastic filaments with an average mechanical property through heated nozzle onto the Cartesian table layer by layer. Deposition of pure metal through FDM is challenging due to the high melting point and viscosity of the metallic melt. Till date, few studies have focused on deposition of metallic powders such as steel. In this study, the optimized percentage of powder and binder system for the deposition of 4606 steel powder using the FDMS process has been developed for the first time.

2 Methodology

2.1 Materials

AISI low-alloy 4605 powder with average particle size of $3/9 \mu\text{m}$ (D_{50}), supplied by Jiangxi Yuean Superfine Metal

(China), was used for the steel powder. The SEM micrograph obtained from this powder is shown in Fig. 1.

The particles were spherical with a wide surface area which increased their density, process ability, and benefits the debinding process (requires less amount of binder). Chemical composition of the powder was characterised using SEM imaging (Tescan Vega) and is presented in Table 2. As the alloy content of the powder was less than 5%, the powder has been categorised as low-alloy steel.

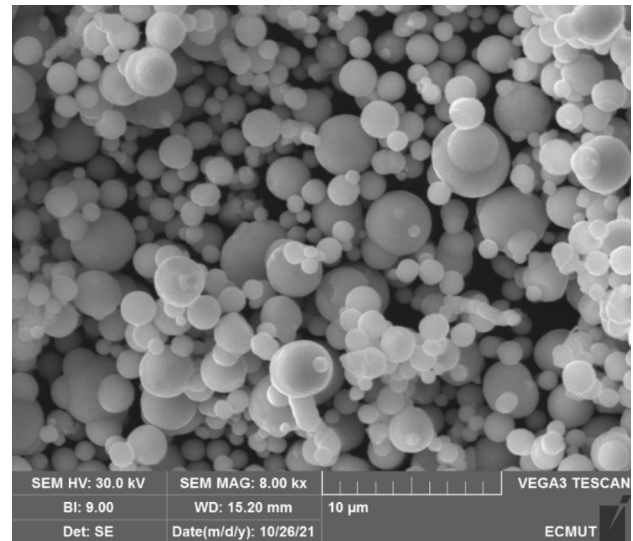


Fig. 1 Scanning electron micrograph of 4605 low-alloy steel

Table 1 Some of the used binder systems in powder injection [6]

Main component (50–90 vol. %)	Backbone (10–50 vol. %)	Additives (1–10 vol. %)
Carnauba wax	Polypropylene (PP)	Stearic acid
Paraffin wax	Ethyl vinyl acetate (EVA)	Stearic acid
Paraffin wax	High density polyethylene (HDPE)	Stearic acid
Paraffin wax	Polyethylene (PE), PP	Stearic acid
Paraffin wax	HDPE, PP, Polystyrene (PS)	Stearic acid
Paraffin wax	PE	Stearic acid, oleic acid
Polyethylene glycol (PEG)	Polymethyl methacrylate (PMMA)	Stearic acid
PEG	Polyvinylbutyral (PVB)	Stearic acid
PEG	Polyethylene wax	Stearic acid
PEG	Polyimide diisocyanate	2, 6-di-tert-butyl-4-hydroxytoluene
Polyoxymethylene (POM)	Low density polyethylene (LDPE)	Stearic acid
POM	Polyolefins	Poly-1,3-dioxepane or poly-1,3-dioxolane or mixtures thereof
POM	PE	Butanediol formal
Agar (gel forming polysaccharide)	Glucose	Deionized water, calcium borate, methyl-p-hydroxybenzoate and propyl-p-hydroxybenzoate as biocides
PEG or polypropylene glycol or polyvinyl alcohol	PS and/or PE	Methylene chloride
Partially hydrolysed cold water soluble polyvinyl alcohol	PE or PP	Glycerin, INT-33PA, steric acid, water

Table 2 Chemical composition of low-alloy 4605 powder

Component	Iron (Fe)	Nickel (Ni)	Molybdenum (Mo)	Carbon (C)	Oxygen (O)
Weight percentage (%)	Balance	1.9–2.1	0.2–0.5	0.4–0.6	≤ 0.45

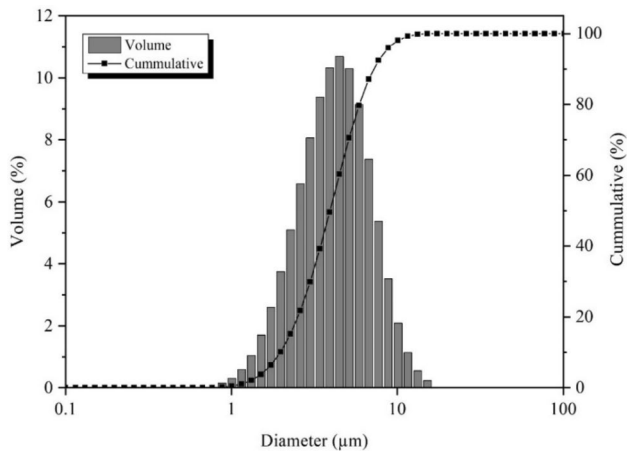


Fig. 2 Particle size distribution of 4605 low-alloy steel powder

Size distribution of the powder was investigated using Particle Size Analyser (HORIBA LA-950V2) ranging from 0.2 to 2000 µm (Fig. 2). As observed, powder size distribution ranged from 1 to 8 µm, and highest volume percentage was dedicated to the particle size of 7.2 µm. In this analysis, D_{10} , D_{50} , and D_{90} as the intercepts for 10, 50 and 90% of the cumulative mass were 1.97, 7.23, and 3.90, respectively.

Size distribution slope parameter (S_w) was measured using Eq. 1 [7].

$$S_w = \frac{2.56}{\log\left(\frac{d_{90}}{d_{10}}\right)} \quad (1)$$

Through an injection process, lower S_w values are more desirable. Lower values of S_w indicate broader range of particle size which result in a smoother injection process. Values higher than 2 result in higher density values, and as a result, less amount of binder is employed. Meanwhile, it should be noticed that the maximum accepted value of S_w in this field is 7. Values higher than 7 result in narrow size distributions which are hardly recommended for injection purposes. Using Eq. 1, the value of S_w in this study was found to be 4.53, which approved the suitability of the powder in this study.

As for the binder system, the selected binder constituents were similar to the approved binder system in the studies of Hnatkova et al. [8], Royer et al. [9], and Yilmaz et al. [10].



Fig. 3 Binder system components

Table 3 Characteristics of the Binder constituents used in this study

Binder	Density (g/cm ³)	Melting range (°C)	Decomposition range (°C)
PW	0.91	58–60	180–320
PP	0.90	160–165	350–470
CW	0.99	83–91	250–440
SA	0.86	70–71	263–306

These constituents consist of paraffin wax (PW) as the major component, polypropylene (PP) as the backbone, carnauba wax (CW) as lubricant and plasticizer and stearic acid (SA) as surfactant (Fig. 3). Density, temperature of melting, and decomposition range of the used binder components are depicted in Table 3.

2.2 Feedstock Preparation

To obtain a homogenous composition, Haake Lab mixer (capacity of 60 cc) was used to mix the binder system components. The operating condition was temperature of 170 °C (based on the highest melting point amongst the components (PP)), mixing rate was 75 rpm for the duration of 20 min. In order to obtain an optimum percentage of each constituent, response surface methodology (RSM) using Design Expert software was used to optimize the strength, density and decrease the viscosity of the feedstock. The range for the constituents derived from two similar studies [11, 12] was chosen to be 20–25% for PP, 10–15% for CW, 55–69% for PW and 1–5% for SA. Overall 15 experiments were obtained as shown in Table 4.

For every feedstock, the optimum percentage of the powder loading has a unique value. Higher the powder loading,

higher the density and mechanical properties of the final metallic part produced. On the other hand, a high powder loading in the feedstock increases the viscosity of the feedstock melt and gives rise to the injection process. In order to find the optimum percentage of the metallic powder inside the feedstock, 25% of PP, 15% of CW, 55% of PW and 5% of SA were mixed inside the Haake Lab mixer (capacity of 60 cc) at the temperature of 170 °C and mixing rate of 75 rpm for 5 min after which 87 wt% of the powder was added and the rotating torque of the mixer was monitored. After 2 min, more amount of powder was added to reach 88 wt%. This step continued till 95 wt% of the metallic powder where the rotating torque was measured at each stage. As observed from Fig. 4, above 92 wt% of powder loading, higher torque value was developed in the mixer. This is due to binder system deficiency which results in higher friction and wear rates [13]. This point is critical weight concentration of powder (CPVC). Adequate amount of binder is generally reported to be 2–5% lower than the CPVC. For this reason, 90% was chosen as the powder loading of 4605 alloy for all designed experiments (binder systems) that was weighted using the Sartorius (BL1500S) digital scale. Figure 5 shows the B1 feedstock sample.

2.3 Printing

The compounded feedstock was extruded into filaments, and then, it was granulated. The feedstock granules were then fed to the hopper of the extruder of a custom-made FDMS machine (Fig. 6), and printing was done using the parameters shown in Table 5. In order to measure the tensile properties of the printed sample, ISO 2740 [14] tensile testing sample was chosen as the geometry of the print.

Table 4 The designed experiments

Sample name	PW	PP	CW	SA
B1	69	20	10	1
B2	59.6	25	10.4	5
B3	59	25	15	1
B4	63.1	21.9	10	5
B5	66.3	21.7	10	2
B6	63.7	20.3	15	1
B7	62.5	25	10	2.5
B8	57	25	13	5
B9	60	20	15	5
B10	60.5	22.2	12.3	5
B11	61.3	25	12.7	1
B12	61.4	22.6	15	1
B13	64.4	20.1	12.1	3.4
B14	58.8	23	15	3.2
B15	64	22.7	12	1.2

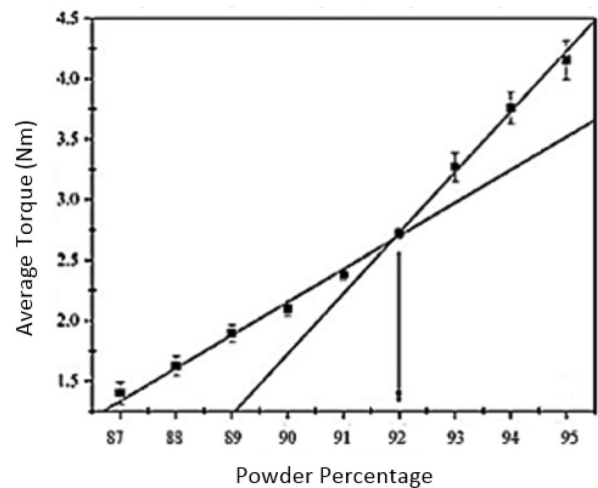


Fig. 4 Mean torque values for different weight percentages of powder

2.4 Debinding and Sintering

In the next step, the samples were debinded in order to remove the excess binder within the green part. Debinding was done in two stages of solvent and thermal debinding. Solvent debinding was done using n-heptane solution at 70 °C for 5 h [15] where SA and PW were partially removed and as a result a porous structure was formed. Product porosity is important at the thermal debinding stage, as it can affect the diffusion of the remaining excess binders.

Thermal debinding and sintering were applied later to remove the excess binder to obtain the brown part. Thermal debinding and sintering were based on the study of Özgün et al. [16]. The heating cycle was rising the temperature from room temperature to 1200 °C with heating rate of 3 °C/min and keeping that temperature for 120 min at argon atmosphere. In Fig. 7, the printed green part as well as the debinded and sintered B1 sample can be observed.

2.5 Sample Characterization

Instron 3211 capillary rheometer with the temperature of 170 °C and L/D of 30 was used to analyse the rheological



Fig. 5 Compounded B1 feedstock sample

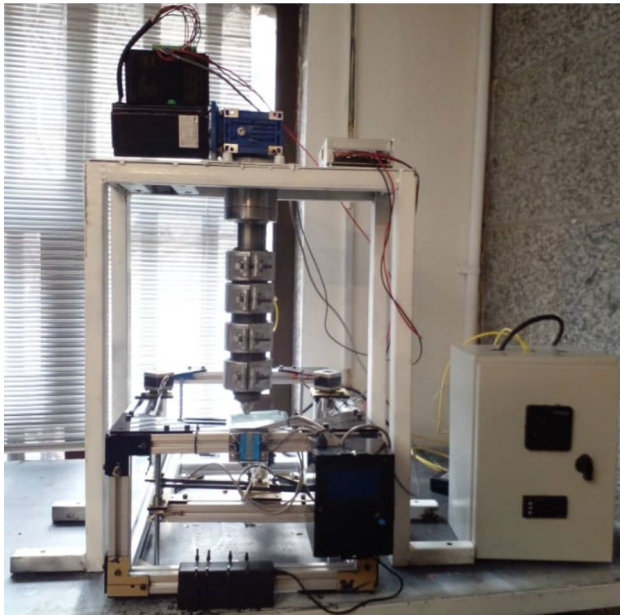


Fig. 6 custom-made FDMS system with feedstock extruder

Table 5 Printing parameters

	Value	Unit
Nominal layer height	0.3	Mm
Printing temperature	170	°C
Line width	0.4	Mm
Wall thickness	1	Mm
Layer height	0.2	Mm
Build plate temperature	90	°C
Print speed	30	mm/s

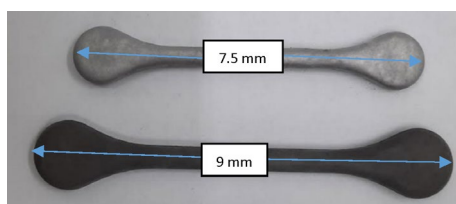


Fig. 7 Final ISO 2740 tensile testing sample obtained from B1 sample

behaviour of the feedstocks. Flow ability state and evaluation of the feedstock were reported based on the outcome of rheological analysis. Density measurement of the sintered samples was carried out using Sartorius CP224S Analytical Balance apparatus following Archimedes method and MPIF 42 standard. Zwick Z50 KN tensile testing machine (German made) was used to perform the tensile testing under displacement control with the speed of 0.1 mm/min at room

Table 6 Steady-state of mixing torque value for different feedstocks

Sample	Mixing torque (N.m)
B1 + 90 wt% of 4605 powder	0.51
B2 + 90 wt% of 4605 powder	1.65
B3 + 90 wt% of 4605 powder	2.1
B4 + 90 wt% of 4605 powder	0.35
B5 + 90 wt% of 4605 powder	0.57
B6 + 90 wt% of 4605 powder	0.98
B7 + 90 wt% of 4605 powder	0.85
B8 + 90 wt% of 4605 powder	1.75
B9 + 90 wt% of 4605 powder	1.62
B10 + 90 wt% of 4605 powder	1.5
B11 + 90 wt% of 4605 powder	1.95
B12 + 90 wt% of 4605 powder	1.88
B13 + 90 wt% of 4605 powder	0.4
B14 + 90 wt% of 4605 powder	1.79
B15 + 90 wt% of 4605 powder	1.73

temperature, according to the MPIF 50 standard. For all of the above-mentioned test, 5 samples were tested and the average result of the five was reported.

3 Results and Discussion

3.1 Rheological Behaviour of Binder System

Flow behaviour of binder system as well as compressibility of the powder are the main factors that are used to validate the mixture process ability. Therefore, rheological studies are essential to predict the process performance. In this study, the stable state mixing torque was measured for each sample which is an indication of flow ability of the feedstock. At the initial stages when the powder is introduced to the binder system inside the mixing chamber, the torque starts to fluctuate and after some time it become stable when homogenized. Table 6 shows the steady-state mixing torque of the mixer for each feedstock batch.

As it is observed from the results, increase in SA and PW inside the binder system results in reduction of steady-state mixing torque which indicates decrease in the viscosity for those samples. B4 and B13 samples (with highest content of SA and PW) has the lowest viscosity. Similar results have been reported for high contents of PW in similar studies [17, 18]. The results of viscosity of feedstock as a function of shear rate, measured at 170 °C, are shown in Table 7. -

Shear rate is directly related to the viscosity of the binder system. Such behaviour is appointed for a non-Newtonian, shear thinning, and pseudo-plastic feedstock [19, 20]. Such

behaviour fits well with processes that require injection and extrusion with minimum jetting as it allows the feedstock to reach fix platen of the FDM machine through a smoother flow.

Comparing the effect of components of binder system on the viscosity, it can be observed that increase in PP content has the highest effect on increasing the viscosity while this is diverse for PW and SA as it can be observed in B4 and B13 samples containing the maximum amount of PW and SA. Overall, in such processes, at shear rates ranging from 100 to 10,000 s⁻¹, viscosity values lower than 1000 Pa.s are highly recommended [21]. Following this reference, all fifteen binder systems designed by RSM in this study are processable and injectable. Relation between viscosity and shear rate was further investigated using Eq. 2 where viscosity, shear rate, power law index (shear rate sensitivity), and constant values were presented as $\eta, \dot{\gamma}, n$, and K , respectively. Shear rate sensitivity (n) was then calculated based on the values in Table 7 which are presented in Table 8.

$$\eta = K\dot{\gamma}^{n-1} \quad (2)$$

Additives such as PW, SA, and CW are found useful in reducing the viscosity to some limit after which the excess amount results in deformation during the debinding process.

3.2 Density and Strength

Actual and theoretical density values for samples B1–B15 are presented in Fig. 8. Theoretical density ranges from 93.12 to 95.79%. B7 and B11 presents the highest density

Table 7 Viscosity of feedstocks at different shear rates

Sample	Shear rate (s ⁻¹)			
	25	100	300	1000
	Viscosity (Pa.s)			
B1 + 90 wt% of 4605 powder	69	20	10	1
B2 + 90 wt% of 4605 powder	59.6	25	10.4	5
B3 + 90 wt% of 4605 powder	59	25	15	1
B4 + 90 wt% of 4605 powder	63.1	21.9	10	5
B5 + 90 wt% of 4605 powder	66.3	21.7	10	2
B6 + 90 wt% of 4605 powder	63.7	20.3	15	1
B7 + 90 wt% of 4605 powder	62.5	25	10	2.5
B8 + 90 wt% of 4605 powder	57	25	13	5
B9 + 90 wt% of 4605 powder	60	20	15	5
B10 + 90 wt% of 4605 powder	60.5	22.2	12.3	5
B11 + 90 wt% of 4605 powder	61.3	25	12.7	1
B12 + 90 wt% of 4605 powder	61.4	22.6	15	1
B13 + 90 wt% of 4605 powder	64.4	20.1	12.1	3.4
B14 + 90 wt% of 4605 powder	58.8	23	15	3.2
B15 + 90 wt% of 4605 powder	64	22.7	12	1.2

Table 8 Shear rate sensitivity values for each binder system

Sample	Shear rate sensitivity (n)
B1	0.67
B2	0.76
B3	0.99
B4	0.58
B5	0.67
B6	0.72
B7	0.70
B8	0.91
B9	0.87
B10	0.80
B11	0.95
B12	0.90
B13	0.54
B14	0.91
B15	0.90

values while B1, B9 and B13 has the lowest densities. B7 and B11 are the samples with the highest content of PP and CW. Therefore, changes in density are linked to the backbone polymer of system. Higher the backbone polymer, higher the density of the final part.

The strength of the final samples measured using the tensile testing machine is shown in Fig. 9. As it can be observed, B7 and B11 have the highest strengths.

3.3 Optimised Feedstock System

After entering the measured responses of each experiment (strength, density and viscosity) to the Design Expert software, with the aim of increasing the strength and density and decreasing of viscosity, it proposed four optimum samples as shown in Table 9 from which the first proposed system with the highest desirability percentage (89.4) was selected.

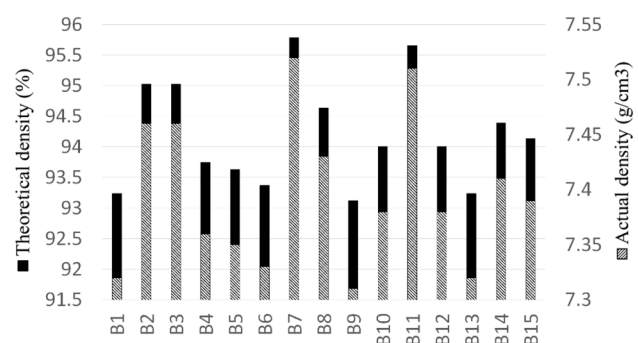
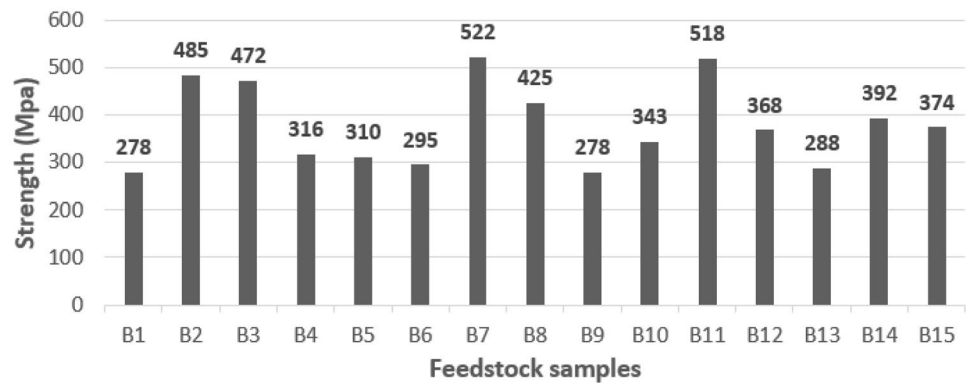


Fig. 8 Actual and theoretical density of samples containing 90% powder

Fig. 9 Yield strength of different samples**Table 9** Optimum binder system predictions of design expert software

Predicted system	PW (wt%)	PP (wt%)	CW (wt%)	SA (wt%)	Desirability (%)
1	61	25	10	4	89.4
2	57.7	25	15	2.3	43.9
3	60.6	22.7	11.7	5	38.8
4	62.4	20	15	2.6	18.2

Therefore, optimum binder system was selected based on 61 wt% of PW, 25 wt% of PP, 10 wt% CW, and 4 wt% SA.

4 Conclusion

In this study, the rheological, physical and mechanical properties of different feedstocks and their final products (brown parts) have been studied to determine an optimum feedstock composition for additive manufacturing of 4605 steel powder. The optimum binder selected consists of 61 wt% of PW, 25 wt% of PP, 10 wt% of CW, and 4 wt% of SA along with 90 wt% of steel powder. This raw material has a viscosity of 1 Pa.s and when turned into brown part, it has strengths of 543 MPa and density of 96.3% of bulk material.

References

- Singh N, Hameed P, Ummethala R, Manivasagam G, Prashanth K, and Eckert J, *Mater Today Adv* **8** (2020) 100097.
- Liu B, Wang Y, Lin Z, and Zhang T, *Mater Lett* **263** (2020) 127252.
- Jurisch M, Studnitzky T, Andersen O, and Kieback B, *Powder Metall* **58** (2015) 339.
- Su Z, Zhang S, Liu L, and Wu J, *J Alloys Compd* **871** (2021) 159569.
- Sa'ude N, Ibrahim M, and Saidin W, *Appl Mech Mater Trans Tech Publ* **315** (2013) 582.
- Gonzalez-Gutierrez J, Cano S, Schuschnigg S, Kukla C, Sapkota J, and Holzer C, *Materials* **11** (2018) 840.
- Sotomayor M E, Várez A, and Levenfeld B, *Powder Technol* **200** (2010) 30–36.
- Hnatkova E, Hausnerova B, and Filip P, *Ceram Int* **45** (2019) 20084.
- Royer A, Barriere T, and Bienvenu Y, *Powder Technol* **336** (2018) 311.
- Yılmaz E, Gökçe A, Findik F, and Gülsoy H Ö, *Vacuum* **142** (2017) 164.
- Ahn S, Park S J, Lee S, Atre S V, and German R M, *Powder Technol* **193** (2009) 162.
- Lin K-H, *Mater Des* **32** (2011) 1273.
- Sanetnik D, Hausnerova B, Novak M, Mukund B N, *3D Print Addit Manuf* (2021).
- ISO 2740, International Standard ISO, vol 2004 (2004).
- Ahmad F, Mohammad M, Muhsan A, Ali M, Naseer A, Aslam M, and Malik M, in *Advances in Material Sciences and Engineering*, (eds) Awang M, Emamian SS, and Yusof F, Springer, Singapore (2020), p 377.
- Özgül Ö, Gülsoy H Ö, Yılmaz R, and Findik F, *J Alloys Compd* **576** (2013) 140.
- Gerling R, Aust E, Limberg W, Pfuff M, and Schimansky F, *Mater Sci Eng A* **423** (2006) 262.
- Thomas-Vielma P, Cervera A, Levenfeld B, and Várez A, *J Eur Ceram Soc* **28** (2008) 763.
- Sotomayor M, Krupa I, Várez A, and Levenfeld B, *Renew Energy* **68** (2014) 140.
- Lin D, Sanetnik D, Cho H, Chung S T, Kwon Y S, Kate K H, Hausnerova B, Atre S V, and Park S J, *Powder Technol* **311** (2017) 357.
- Izadbakhsh H, Sheikh H, Sharifi E M, Sardarian M, Loghman-Estarki M, and Ramazani M, *Ceram Int* **47** (2021) 25932.

Publisher's Note Springer Nature remains neutral with regard to jurisdictional claims in published maps and institutional affiliations.